**

受動性に基づく非線形視覚フィードバック制御 – 安定性と L_2 ゲイン制御性能の解析*

丸山 章 †・河合 宏之 ‡・藤田 政之 §

Passivity-based Visual Feedback Control of Nonlinear Mechanical Systems – Stability and L_2-Gain Performance Analysis*

Akira MARUYAMA†, Hiroyuki KAWAI‡ and Masayuki FUJITA§

This paper investigates the relative rigid body motion (positions and rotations) control problem with visual information. Firstly the model of the relative rigid body motion and the nonlinear observer are considered in order to derive the visual feedback system. Secondly stability and L_2-gain performance analysis are discussed based on passivity. Finally we present simulation results to confirm the effectiveness of the proposed visual feedback control design.

1. Introduction

Vision based control of robotic systems involves the fusion of robot kinematics, dynamics, and computer vision system to control the position of the robot end-effector in an efficient manner. The combination of mechanical control with visual information, so-called *visual feedback control* or *visual servo*, should become extremely important, when we consider a mechanical system working under *dynamical* environments. Recent research efforts toward this direction have been nicely collected in Ref. [1,2].

This paper deals with the relative rigid body motion control of a moving target object with respect to the camera frame. This control problem is standard and important, and has gained much attention of researchers for many years [3–7]. The control objective is to track the moving target object in a three-dimensional workspace by image information. The typical example is shown in Fig. 1. Hence the dynamics of the relative rigid body motion is described by the nonlinear systems in a 3-D workspace. Kelly et al. [6] have considered a simple image-based controller for the 3-D visual feedback system under the assumption that the objects' depths are known. Their controller has guaranteed that the overall closed-loop system is stable by invoking the Lyapunov direct method. Shakernia et al. [7] have derived the visual feedback controller for an Unmanned Air Vehicle in the 3-D workspace and shown a detailed stability analysis of the closed-loop system. Several approaches have been proposed to guarantee global stability [8–10]. In the area of vision and control, it has been expected to investigate not only stability but analytical techniques based on theoretical approaches [2]. Since one of the control objective is to track the moving target object, the tracking performance measure is important for the 3-D visual feedback systems. However, performance measures for the 3-D visual feedback systems have not been obtained in the previous works.

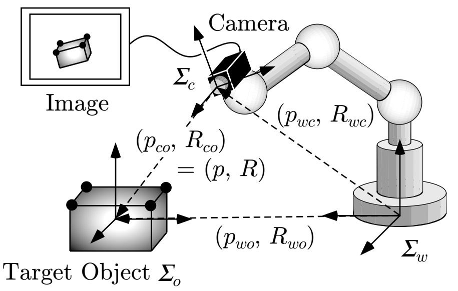

Fig. 1 Eye-in-Hand visual feedback system

* **2001 年 9 月 3 日

† （株）不二越 ロボット開発部 Nachi-Fujikoshi Corp.; 1-1-1 Fujikoshihonmachi, Toyama city, Toyama 930-8511, JAPAN

‡ 金沢大学 大学院 自然科学研究科 Graduate School of Natural Science and Technology, Kanazawa University; 2-40-20 Kodatsuno, Kanazawa city, Ishikawa 920-8667, JAPAN

§ 金沢大学 工学部 Faculty of Engineering, Kanazawa University; 2-40-20 Kodatsuno, Kanazawa city, Ishikawa 920-8667, JAPAN

Key Words: visual feedback control, passivity, Lyapunov stability, L_2-gain performance analysis, nonlinear control.

In this paper, we discuss stability and L_2-gain performance analysis for the full 3-D visual feedback system based on passivity from the theoretical standpoint. In order to derive the full 3-D visual feedback system, we will consider a relative rigid body motion dynamics and propose a nonlinear observer. The key idea of this paper is to utilize an error function of the rotation matrix as a Lyapunov or storage functions. This approach continues the research originally presented in Ref. [11–13]. While the previous work have investigated the image-based visual feedback control of the planar motion types, this work deals with the position-based visual feedback control for 3-D visual feedback systems.

This paper is organized as follows. In Section **2**, we consider a model of the relative rigid body motion. Section **3** shows a nonlinear observer which estimates the relative rigid body motion. The main theorem concerned with stability is derived in Section **4**, and L_2-gain performance analysis is discussed in Section **5**. In Section **6**, we present the simulation results. Finally, we offer some conclusions in Section **7**.

Let a rotation matrix $R_{ab}\in\mathcal{R}^{3\times 3}$ represent the change of the principle axes of a frame b relative to a frame a. Then, R_{ab} is known to become orthogonal with unit determinant. Such a matrix belongs to a Lie group of dimension three, called $SO(3)=\{R_{ab}\in\mathcal{R}^{3\times 3}|R_{ab}R_{ab}^{\rm T}=R_{ab}^{\rm T}R_{ab}=I,\det(R_{ab})=+1\}$. The configuration space of the rigid body motion is the product space of $\mathcal{R}^3$ with $SO(3)$, which should be denoted as $SE(3)$ throughout this paper (see, e.g. [14]).

2. Relative Rigid Body Motion

2.1 Relative Rigid Body Motion Model

We consider the eye-in-hand system [1] depicted in Fig. 1, where the coordinate frame Σ_w represents the world frame, Σ_c represents the camera (end-effector) frame, and Σ_o represents the object frame, respectively. Let $p_{co}\in\mathcal{R}^3$ and $R_{co}\in\mathcal{R}^{3\times 3}$ denote the position vector and the rotation matrix from the camera frame Σ_c to the object frame Σ_o. Then, the relative rigid body motion from Σ_c to Σ_o can be represented by $(p_{co},R_{co})\in SE(3)$. Similarly, we will define the rigid body motion (p_{wc},R_{wc}) from Σ_w to Σ_c, and (p_{wo},R_{wo}) from Σ_w to Σ_o, respectively, as in Fig. 1.

The objective of the visual feedback control is to bring the actual relative rigid body motion (p_{co},R_{co}) to a given reference (p_d,R_d) (see, e.g. [1]). Our goal is to determine the camera's motion via the visual information for this purpose. The reference (p_d,R_d) for the rigid motion (p_{co},R_{co}) is assumed to be constant in the paper.

In this subsection, let us derive a model of the relative rigid body motion. The rigid body motion (p_{wo},R_{wo}) of the target object, relative to the world frame Σ_w, is given by

$$p_{wo}=p_{wc}+R_{wc}p_{co} \tag{1}$$
$$R_{wo}=R_{wc}R_{co} \tag{2}$$

which is a direct consequence of a transformation of the coordinates in Fig. 1. These coordinate transformations can be found in Ref. [14] (Chap.2, Eq.(2.3) and (2.22)). Using the property of a rotation matrix, i.e. $R^{-1}=R^{\rm T}$, the rigid body motion (1) and (2) is now rewritten as

$$p_{co}=R_{wc}^{\rm T}(p_{wo}-p_{wc}) \tag{3}$$
$$R_{co}=R_{wc}^{\rm T}R_{wo}. \tag{4}$$

The dynamic model of the relative rigid body motion involves the velocity of each rigid body. To this aid, let us consider the velocity of a rigid body as described in Ref. [14]. Let $\hat{\omega}_{wc}$ and $\hat{\omega}_{wo}$ denote the instantaneous body angular velocities from Σ_w to Σ_c, and from Σ_w to Σ_o, respectively [14] (Chap.2, Eq.(2.49)). Here the operator '$\wedge$' (wedge), from $\mathcal{R}^3$ to the set of 3×3 skew-symmetric matrices $so(3)$, is defined as

$$\hat{a}=(a)^{\wedge}:=\begin{bmatrix}0 & -a_3 & a_2\\ a_3 & 0 & -a_1\\ -a_2 & a_1 & 0\end{bmatrix},\quad a=\begin{bmatrix}a_1\\ a_2\\ a_3\end{bmatrix}.$$

The operator '$\vee$' (vee) denotes the inverse operator to '$\wedge$': i.e., $so(3)\to\mathcal{R}^3$. Recall that a skew-symmetric matrix corresponds to an axis of rotation (via the mapping $a\mapsto\hat{a}$). With these, it is possible to specify the velocities of each rigid body as follows [14] (Chap.2, Eq.(2.55)).

$$\dot{p}_{wc}=R_{wc}v_{wc},\quad \dot{R}_{wc}=R_{wc}\hat{\omega}_{wc} \tag{5}$$
$$\dot{p}_{wo}=R_{wo}v_{wo},\quad \dot{R}_{wo}=R_{wo}\hat{\omega}_{wo}. \tag{6}$$

Note that the above formula will be utilized in **Appendix 1**.

Differentiating (3) and (4) with respect to time, we can obtain

$$\dot{p}_{co}=-v_{wc}+\hat{p}_{co}\omega_{wc}+R_{co}v_{wo} \tag{7}$$
$$\dot{R}_{co}=-\hat{\omega}_{wc}R_{co}+R_{co}\hat{\omega}_{wo} \tag{8}$$

where detailed derivation can be found in **Appendix 1**. Now, let us denote the body velocity of the camera relative to the world frame Σ_w as

$$u_c:=[v_{wc}^{\rm T}\ \omega_{wc}^{\rm T}]^{\rm T}. \tag{9}$$

Further, the body velocity of the target object relative to Σ_w should be denoted as

$$V_{wo}:=[v_{wo}^{\rm T}\ \omega_{wo}^{\rm T}]^{\rm T}. \tag{10}$$

Then we can rearrange the above eqs. (7) and (8) in a matrix form as follows.

$$\begin{bmatrix}\dot{p}\\ (\dot{R}R^{\rm T})^{\vee}\end{bmatrix}=\begin{bmatrix}-I & \hat{p}\\ 0 & -I\end{bmatrix}u_c+\begin{bmatrix}R & 0\\ 0 & R\end{bmatrix}V_{wo}. \tag{11}$$

Here (p,R) denotes (p_{co},R_{co}) for short. The eq. (11) should be the model of the relative rigid body motion.

2.2 Property of Relative Rigid Body Motion

Let us define the error of the relative rigid body motion as

$$(p_{er}, R_{er}) := (p - p_d, RR_d^{\mathrm{T}}) \tag{12}$$

where the reference of the relative rigid body motion (p_d, R_d) is assumed to be constant. Note that $p = p_d$ and $R = R_d$ iff $p_{er} = 0$ and $R_{er} = I$.

From the eqs. (11) and (12) with the property of '$\wedge$' (wedge) (i.e., $\hat{a}^{\mathrm{T}} = -\hat{a}$, $a \in \mathcal{R}^3$), the error equation of the relative rigid body motion can be given by

$$\begin{bmatrix} \dot{p}_{er} \\ (\dot{R}_{er} R_{er}^{\mathrm{T}})^{\vee} \end{bmatrix} = -B^{\mathrm{T}}(p) u_c + \begin{bmatrix} R & 0 \\ 0 & R \end{bmatrix} V_{wo} \tag{13}$$

where B is defined as

$$B(a) = \begin{bmatrix} I & 0 \\ \hat{a} & I \end{bmatrix}$$

for any vector $a \in \mathcal{R}^3$. Let the matrix $\mathrm{sk}(R)$ denote $\frac{1}{2}(R - R^{\mathrm{T}})$ and let

$$e_R(R) := \mathrm{sk}(R)^{\vee} \tag{14}$$

represent an error vector of the rotation matrix R. Further, we define an error vector of the relative rigid body motion as follows.

$$e_r := \left[\, p_{er}^{\mathrm{T}} \;\; e_R^{\mathrm{T}}(R_{er}) \,\right]^{\mathrm{T}}. \tag{15}$$

It should be noted that $e_r = 0$ provided $p_{er} = 0$ and $R_{er} = I$. Then the following lemma can be obtained.

[**Lemma 1**] If the target object is static, i.e. $V_{wo} = 0$, and $e_r(0) = 0$, then for the system (13), we have

$$\int_0^T u_c^{\mathrm{T}} \nu_c dt \geq 0, \; \forall T > 0 \tag{16}$$

where ν_c is defined by

$$\nu_c = -B(p_d) e_r. \tag{17}$$

(Proof) Consider the positive definite function defined as

$$V_c = \frac{1}{2}\|p_{er}\|^2 + \phi(R_{er}) \tag{18}$$

where ϕ is the error function of the rotation matrix and important for our proposed scheme. We refer to **Appendix 2** for this error function on $SO(3)$.

From the property of '$\wedge$' (wedge), i.e. '$\wedge$' is the cross product operator and $\hat{a}$ is a 3×3 skew-symmetric matrix, we have $p_{er}^{\mathrm{T}} \hat{p}_{er} \omega_{wc} = -p_{er}^{\mathrm{T}} \hat{\omega}_{wc} p_{er} = 0$.

Using this fact and evaluating the time derivative of V_c gives us

$$\begin{aligned} \dot{V}_c &= p_{er}^{\mathrm{T}} \dot{p}_{er} + e_R^{\mathrm{T}}(R_{er})(\dot{R}_{er} R_{er}^{\mathrm{T}})^{\vee} \\ &= e_r^{\mathrm{T}} \begin{bmatrix} \dot{p}_{er} \\ (\dot{R}_{er} R_{er}^{\mathrm{T}})^{\vee} \end{bmatrix} = -e_r^{\mathrm{T}} B^{\mathrm{T}}(p_d + p_{er}) u_c \\ &= -e_r^{\mathrm{T}} B^{\mathrm{T}}(p_d) u_c + p_{er}^{\mathrm{T}} \hat{p}_{er} \omega_{wc} \\ &= -e_r^{\mathrm{T}} B^{\mathrm{T}}(p_d) u_c - p_{er}^{\mathrm{T}} \hat{\omega}_{wc} p_{er} = -e_r^{\mathrm{T}} B^{\mathrm{T}}(p_d) u_c \\ &= u_c^{\mathrm{T}} \nu_c. \end{aligned} \tag{19}$$

Since $e_r(0) = 0$, we have $V_c(0) = 0$. Integrating the eq. (19) from 0 to T yields

$$\int_0^T u_c^{\mathrm{T}} \nu_c dt = V_c(T) - V_c(0) = V_c(T) \geq 0. \tag{20}$$

This completes the proof. **

(Remark 1) In the error equation of the relative rigid body motion (13), $p_{er}^{\mathrm{T}} \hat{\omega}_{wc} p_{er} = 0$ holds. This property is analogous to the one of the robot dynamics, i.e. $x^{\mathrm{T}}(\dot{M} - 2C)x = 0$, $\forall x \in \mathcal{R}^m$ (where $M \in \mathcal{R}^{m \times m}$ is the manipulator inertia matrix and $C \in \mathcal{R}^{m \times m}$ is the Coriolis matrix [14]). Moreover, let us take the body velocity of the camera u_c as the input and ν_c as its output. Then, **Lemma 1** would suggest that the system (13) is *passive* from the input u_c to the output ν_c just formally as in the definition in Ref. [15].

3. Nonlinear Observer Design

The visual feedback control task should require information of the relative rigid body motion (p, R). However, the measurable information is only the one of image in the visual feedback systems. Hence, we consider a nonlinear observer which estimates the relative rigid body motion using information of the image.

First, we shall consider the following dynamic model which just comes from the actual relative rigid body motion model (11).

$$\begin{bmatrix} \dot{\bar{p}} \\ (\dot{\bar{R}} \bar{R}^{\mathrm{T}})^{\vee} \end{bmatrix} = \begin{bmatrix} -I & \hat{\bar{p}} \\ 0 & -I \end{bmatrix} u_c + \begin{bmatrix} I & 0 \\ 0 & \bar{R} \end{bmatrix} u_e \tag{21}$$

where $(\bar{p}, \bar{R})$ is the estimated value of the relative rigid body motion. The new input u_e is to be determined in order to converge the estimated value to the actual relative rigid body motion. Because the design of u_e needs a property of the whole visual feedback system, we will propose u_e with u_c in Section **4**.

Next let us derive a model of a pinhole camera as shown in Fig. 2.

Let λ be a focal length. Let p_{oi} and p_{ci} be coordinates of the target object's i-th feature point relative to Σ_o and Σ_c, respectively. Using a transformation

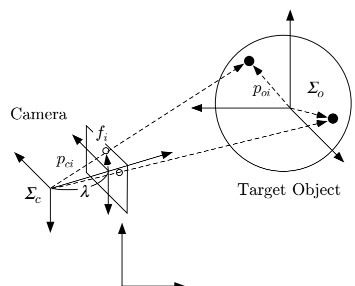

Fig. 2 Pinhole camera

of the coordinates, we have

$$p_{ci} = p + Rp_{oi}. \tag{22}$$

The perspective projection of the i-th feature point onto the image plane gives us the image plane coordinate f_i as follows.

$$f_i = \frac{\lambda}{z_{ci}} \begin{bmatrix} x_{ci} \\ y_{ci} \end{bmatrix} \tag{23}$$

where $p_{ci} := [x_{ci}\ y_{ci}\ z_{ci}]^{\mathrm{T}}$.

It is straightforward to extend this model to the n image points case by simply stacking the vectors of the image plane coordinate, i.e. $f := [f_1^{\mathrm{T}} \cdots f_n^{\mathrm{T}}]^{\mathrm{T}} \in \mathcal{R}^{2n}$. Then the camera model can be expressed by the mapping $\pi : SE(3) \to \mathcal{R}^{2n}$

$$f = \pi(p, R) \tag{24}$$

where π is defined through the eqs. (22) and (23).

Now, we define the estimation error between the estimated value $(\bar{p}, \bar{R})$ and the actual relative rigid motion (p, R) as

$$(p_{ee}, R_{ee}) := (p - \bar{p}, \bar{R}^{\mathrm{T}} R). \tag{25}$$

As is already noted that, if $p = \bar{p}$ and $R = \bar{R}$, then it follows $p_{ee} = 0$ and $R_{ee} = I$. Using the notation $e_R(R)$ defined in the eq. (14), the vector of the estimation error is given by

$$e_e := \left[\, p_{ee}^{\mathrm{T}}\ e_R^{\mathrm{T}}(R_{ee}) \,\right]^{\mathrm{T}}. \tag{26}$$

Note that $e_e = 0$ iff $p_{ee} = 0$ and $R_{ee} = I$.

Next, we will derive the measurement equation from the camera model (24). Suppose the estimation error is *small* enough that we can let $R_{ee} \simeq I + \mathrm{sk}(R_{ee})$, then the eq. (22) becomes

$$p_{ci} = \bar{p}_{ci} - \bar{R}\hat{p}_{oi} e_R(R_{ee}) + p_{ee} \tag{27}$$

where $\bar{p}_{ci} := \bar{p} + \bar{R}p_{oi}$ and the above equation has been described in more detail in **Appendix 3**.

Using Taylor expansion, the first order approximation of the eq. (23) is

$$f_i = \bar{f}_i + \begin{bmatrix} \dfrac{\lambda}{\bar{z}_{ci}} & 0 & -\dfrac{\lambda \bar{x}_{ci}}{\bar{z}_{ci}^2} \\ 0 & \dfrac{\lambda}{\bar{z}_{ci}} & -\dfrac{\lambda \bar{y}_{ci}}{\bar{z}_{ci}^2} \end{bmatrix} (p_{ci} - \bar{p}_{ci}) \tag{28}$$

where $\bar{p}_{ci} = [\bar{x}_{ci}\ \bar{y}_{ci}\ \bar{z}_{ci}]^{\mathrm{T}}$ and $\bar{f}_i := \dfrac{\lambda}{\bar{z}_{ci}} [\bar{x}_{ci}\ \bar{y}_{ci}]^{\mathrm{T}}$.

Assumption 1 The error of the approximation in the eq. (28) is negligible.

(Remark 2) Assumption 1 holds in the neighborhood of the equilibrium point, although this approximation may be an obstacle to guarantee global stability [8–10]. If the initial error is large, a path planning approach [16] will be also effective in our proposed framework.

Under Assumption 1, an approximation of the nonlinear function π around the estimated value $(\bar{p}, \bar{R})$ then is given by

$$f - \bar{f} = J(\bar{p}, \bar{R}) e_e. \tag{29}$$

The matrix $J(\bar{p}, \bar{R}) : SE(3) \to \mathcal{R}^{2n \times 6}$ is defined as

$$J(\bar{p}, \bar{R}) := \begin{bmatrix} L_1(\bar{p}, \bar{R}) \\ L_2(\bar{p}, \bar{R}) \\ \vdots \\ L_n(\bar{p}, \bar{R}) \end{bmatrix} \tag{30}$$

$$L_i(\bar{p}, \bar{R}) := \begin{bmatrix} \dfrac{\lambda}{\bar{z}_{ci}} & 0 & -\dfrac{\lambda \bar{x}_{ci}}{\bar{z}_{ci}^2} \\ 0 & \dfrac{\lambda}{\bar{z}_{ci}} & -\dfrac{\lambda \bar{y}_{ci}}{\bar{z}_{ci}^2} \end{bmatrix} \left[\, I,\ -\bar{R}\hat{p}_{oi} \,\right], \quad i = 1, \cdots, n \tag{31}$$

where $[\bar{x}_{ci}\ \bar{y}_{ci}\ \bar{z}_{ci}]^{\mathrm{T}} = \bar{p} + \bar{R}p_{oi}$. Note that the matrix $J(\bar{p}, \bar{R})$ is like as the image Jacobian which plays an important role in many researches of the visual feedback control [1].

The following assumption will be made.

Assumption 2 For all $(\bar{p}, \bar{R}) \in SE(3)$, the matrix $J(\bar{p}, \bar{R})$ is full column rank.

Under Assumption 2, the relative rigid body motion can be uniquely defined by the image feature vector. Because Assumption 2 may not hold in some cases when $n = 3$, it is known that $n \geq 4$ is desirable for the full column rank of the image Jacobian [17].

The above discussion shows that we can derive the vector of the estimation error e_e from image information f and the estimated value of the relative rigid body motion $(\bar{p}, \bar{R})$,

$$e_e = J^{\dagger}(\bar{p}, \bar{R})(f - \bar{f}) \tag{32}$$

where $\dagger$ denotes the pseudo-inverse. Therefore the estimation error e_e can be exploited in the 3D visual feedback control law using image information f obtained from the camera.

4. Visual Feedback Control

4.1 Visual Feedback Control Problem

In this paper, we rigorously discuss stability and control performance analysis of the visual feedback system with the nonlinear observer.

Let us derive a model of the visual feedback system. First, we define the control error as follows.

$$(p_{ec}, R_{ec}) := (\bar{p} - p_d, \bar{R}R_d^{\mathrm{T}}) \tag{33}$$

which represents the error between the estimated value $(\bar{p}, \bar{R})$ and the reference of the relative rigid body motion (p_d, R_d). It should be remarked that $p_d = \bar{p}$ and $R_d = \bar{R}$ iff $p_{ec} = 0$ and $R_{ec} = I$.

Using the notation $e_R(R)$, the vector of the control error is defined as

$$e_c := \left[\, p_{ec}^{\mathrm{T}}\ e_R^{\mathrm{T}}(R_{ec}) \,\right]^{\mathrm{T}}. \tag{34}$$

Note that $e_c = 0$ iff $p_{ec} = 0$ and $R_{ec} = I$.

From the eqs. (21) and (33), the state equation of the control error can be given by

$$\begin{bmatrix} \dot{p}_{ec} \\ (\dot{R}_{ec}R_{ec}^{\mathrm{T}})^{\vee} \end{bmatrix} = \begin{bmatrix} -I & \hat{\bar{p}} \\ 0 & -I \end{bmatrix} u_c + R_1 u_e \tag{35}$$

where $R_1 = \mathrm{diag}\{I, \bar{R}\}$.

Next, we consider the state equation of the estimation error. Using the eqs. (11), (21) and (25), the state equation of the estimation error can be obtained as follows.

$$\begin{bmatrix} \dot{p}_{ee} \\ (\dot{R}_{ee}R_{ee}^{\mathrm{T}})^{\vee} \end{bmatrix} = \begin{bmatrix} 0 & \hat{p}_{ee} \\ 0 & 0 \end{bmatrix} u_c - u_e + R_2 V_{wo} \tag{36}$$

where $R_2 = \mathrm{diag}\{R, R_{ee}\}$ and more detail of the derivation is shown in **Appendix 4**.

Using the eqs. (35) and (36), the state equation of the visual feedback system can be derived as

$$\begin{bmatrix} \dot{p}_{ec} \\ (\dot{R}_{ec}R_{ec}^{\mathrm{T}})^{\vee} \\ \dot{p}_{ee} \\ (\dot{R}_{ee}R_{ee}^{\mathrm{T}})^{\vee} \end{bmatrix} = \begin{bmatrix} -I & \hat{\bar{p}} & I & 0 \\ 0 & -I & 0 & \bar{R} \\ 0 & \hat{p}_{ee} & -I & 0 \\ 0 & 0 & 0 & -I \end{bmatrix} u + \begin{bmatrix} 0 \\ R_2 \end{bmatrix} V_{wo} \tag{37}$$

where

$$u := \begin{bmatrix} u_c^{\mathrm{T}} & u_e^{\mathrm{T}} \end{bmatrix}^{\mathrm{T}} \tag{38}$$

denotes the control input.

Let us define the error vector of the visual feedback system as

$$e := \begin{bmatrix} e_c^{\mathrm{T}} & e_e^{\mathrm{T}} \end{bmatrix}^{\mathrm{T}} \tag{39}$$

which contains of the control error vector e_c and the estimation error vector e_e. It should be noted that the actual relative rigid body motion (p, R) tends to the reference (p_d, R_d) when $e \to 0$.

Henceforth, we regard the error vector e as the controlled output. Then the visual feedback control problem can be formulated as follows.

Problem: Given $\gamma > 0$, find a control input u such that the closed-loop system satisfies the control objectives as follows:

(1) (Internal stability)
If the target object is static, i.e. $V_{wo} = 0$, then the equilibrium point $e = 0$ for the closed-loop system is asymptotically stable.

(2) (L_2-gain performance analysis)
The closed-loop system has L_2-gain $\leq \gamma$.

Here if the positive constant γ can be sufficient small, then we are able to obtain the extremely small output e for any V_{wo}. Furthermore, if the controlled output tends to zero, i.e. $e \to 0$, then $(p, R) \to (p_d, R_d)$.

4.2 Visual Feedback Control Algorithm and Internal Stability Analysis

Before deriving the visual feedback control algorithm, we show an important lemma.

[**Lemma 2**] If $V_{wo} = 0$ and $e(0) = 0$, then the system (37) satisfies

$$\int_0^T u^{\mathrm{T}} \nu d\tau \geq 0, \quad \forall T > 0 \tag{40}$$

where ν is

$$\nu := \begin{bmatrix} -B(p_d) & 0 \\ R_1^{\mathrm{T}} & -I \end{bmatrix} e. \tag{41}$$

(Proof) Consider the following positive definite function

$$V = \frac{1}{2}\|p_{ec}\|^2 + \phi(R_{ec}) + \frac{1}{2}\|p_{ee}\|^2 + \phi(R_{ee}) \tag{42}$$

which utilizes the error function ϕ. The positive definiteness of the function V can be given by the property of the error function ϕ. Differentiating (42) with respect to time yields

$$\dot{V} = e^{\mathrm{T}} \begin{bmatrix} \dot{p}_{ec} \\ (\dot{R}_{ec}R_{ec}^{\mathrm{T}})^{\vee} \\ \dot{p}_{ee} \\ (\dot{R}_{ee}R_{ee}^{\mathrm{T}})^{\vee} \end{bmatrix}. \tag{43}$$

Observing that the skew-symmetry of the matrices $\hat{p}_{ec}$ and $\hat{p}_{ee}$, i.e. $p_{ec}^{\mathrm{T}}\hat{p}_{ec}\omega_{wc} = -p_{ec}^{\mathrm{T}}\hat{\omega}_{wc}p_{ec} = 0$ and $p_{ee}^{\mathrm{T}}\hat{p}_{ee}\omega_{wc} = -p_{ee}^{\mathrm{T}}\hat{\omega}_{wc}p_{ee} = 0$, the above equation along the trajectories of the system (37) can be transformed into

$$\begin{aligned} \dot{V} &= e^{\mathrm{T}} \begin{bmatrix} -I & \hat{\bar{p}} & I & 0 \\ 0 & -I & 0 & \bar{R} \\ 0 & \hat{p}_{ee} & -I & 0 \\ 0 & 0 & 0 & -I \end{bmatrix} u = e^{\mathrm{T}} \begin{bmatrix} -B^{\mathrm{T}}(p_d) & R_1 \\ 0 & -I \end{bmatrix} u \\ &= u^{\mathrm{T}}\nu. \end{aligned} \tag{44}$$

From $e(0) = 0$, $V(0) = 0$ can be derived. Integrating the eq. (44) from 0 to T, we can obtain

$$\int_0^T u^{\mathrm{T}} \nu d\tau = V(T) - V(0) = V(T) \geq 0. \tag{45}$$

This completes the proof. **

It is well known that there is a direct link between passivity and Lyapunov stability. Thus, we propose the following control input.

$$u = -\begin{bmatrix} K_c & 0 \\ 0 & K_e \end{bmatrix} \nu \tag{46}$$

where K_c and K_e are 6×6 positive definite matrices called the control gain and the estimation gain, respectively. The block diagram of the visual feedback system is shown in Fig. 3.

The result with respect to asymptotic stability of the proposed control input (46) can be established as follows.

[**Theorem 1**] If $V_{wo} = 0$, then the equilibrium point $e = 0$ for the closed-loop system (37) and (46) is asymptotically stable.

(Proof) In the proof of **Lemma 2**, we have already derived that the time derivative of V along the trajectory of the system (37) is formulated as the eq.

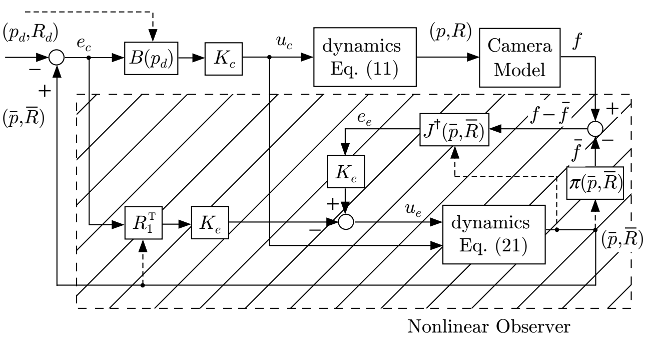

Fig. 3 Block diagram of the visual feedback system

(44). Using the control input (46), the eq. (44) can be transformed into

$$\dot{V} = -e^{\mathrm{T}} K e \tag{47}$$

where K is defined as

$$K := \begin{bmatrix} B^{\mathrm{T}}(p_d) & -R_1 \\ 0 & I \end{bmatrix} \begin{bmatrix} K_c & 0 \\ 0 & K_e \end{bmatrix} \begin{bmatrix} B(p_d) & 0 \\ -R_1^{\mathrm{T}} & I \end{bmatrix}.$$

This completes the proof. **

In the proof of **Theorem 1**, the positive definite function V plays the role of a Lyapunov function.

(Remark 3) **Lemma 2** can be interpreted as follows: The visual feedback system (37) is *passive* from the input u to the output ν just formally as in the definition in Ref. [15].

5. L_2-Gain Performance Analysis

In this section, we consider L_2-gain performance analysis of the visual feedback system. Now, let us define

$$P := K - \frac{1}{2} \begin{bmatrix} I & 0 \\ 0 & \left(1 + \frac{1}{\gamma^2}\right) I \end{bmatrix} \tag{48}$$

where $\gamma \in \mathcal{R}$ is positive. Then we have the following theorem.

[**Theorem 2**] Given a positive scalar γ and consider the control input (46) with the gains K_c and K_e such that the matrix P is positive semi-definite, then the closed-loop system (37) and (46) has L_2-gain $\le \gamma$.

(Proof) Differentiating the positive definite function V defined in the eq. (42) along the trajectory of the closed-loop system and completing the squares yields

$$\begin{aligned} \dot{V} &= -e^{\mathrm{T}} K e + e^{\mathrm{T}} \begin{bmatrix} 0 \\ R_2 \end{bmatrix} V_{wo} \\ &= \frac{\gamma^2}{2} \|V_{wo}\|^2 - \frac{1}{2}\|e\|^2 - \frac{\gamma^2}{2} \left\| V_{wo} - \frac{1}{\gamma^2}[0 \ R_2^{\mathrm{T}}] e \right\|^2 \\ &\quad - e^{\mathrm{T}} K e + \frac{1}{2\gamma^2} e^{\mathrm{T}} \begin{bmatrix} 0 & 0 \\ 0 & I \end{bmatrix} e + \frac{1}{2}\|e\|^2. \end{aligned} \tag{49}$$

Then the velocity of the target object (in the worst case) should be derived as

$$V_{wo} = \frac{1}{\gamma^2} \left[\, 0 \ \ R_2^{\mathrm{T}} \,\right] e. \tag{50}$$

Hence for any V_{wo} it can be verified that the inequality

$$\dot{V} + \frac{1}{2}\|e\|^2 - \frac{\gamma^2}{2}\|V_{wo}\|^2 \le -e^{\mathrm{T}} P e \le 0 \tag{51}$$

holds if P is positive semi-definite. Integrating the eq. (51) from 0 to T and noticing $V(T) \ge 0$, we have

$$\int_0^T \|e\|^2 dt \le \gamma^2 \int_0^T \|V_{wo}\|^2 dt + 2V(0), \ \forall T > 0. \tag{52}$$

This completes the proof. **

The positive definite function V plays the role of the storage function for L_2-gain performance analysis.

6. Numerical Examples

This section presents simulation results to confirm the effectiveness of the proposed visual feedback control design. The performance of the controller can be measured using L_2-gain in the proposed approach, while global stability [8–10] may not be guaranteed.

Let the target object have nine feature points as in Fig. 4 and move as the following:

$$\begin{aligned} &0 \le t < 4: \\ &\quad p_{wo}(t) = [0.25\sin(2\pi t) \ 0.25\sin(2\pi t) \\ &\qquad\qquad 1 + 0.25\sin(2\pi t)]^{\mathrm{T}} \ (\mathrm{m}) \\ &\quad R_{wo}(t) = e^{(\pi/8[\sin(2\pi t) \ \cos(2\pi t) \ \cos(2\pi t)]^{\mathrm{T}})^{\wedge}} \\ &4 \le t \le 8: \\ &\quad p_{wo}(t) = [0 \ 0 \ 1]^{\mathrm{T}} \ (\mathrm{m}) \\ &\quad R_{wo}(t) = e^{([0 \ \pi/8 \ \pi/8]^{\mathrm{T}})^{\wedge}}. \end{aligned}$$

Here (p_{wo}, R_{wo}) represents the position and the rotation of the center point of the nine feature points in Fig. 4.

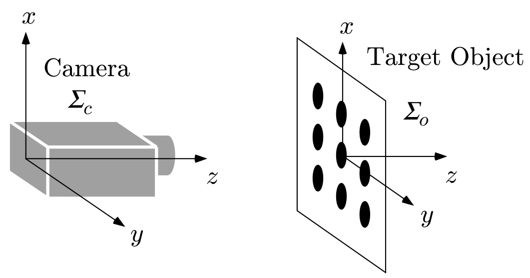

Fig. 4 Simulation condition

Let us consider initial positions and rotations of the camera $(p_{wc}(0), R_{wc}(0))$ and the estimated value $(\bar{p}(0), \bar{R}(0))$ as follows

$$\begin{aligned} p_{wc}(0) &= [0 \ 0 \ 0]^{\mathrm{T}} \ (\mathrm{m}), \ R_{wc}(0) = I \\ \bar{p}(0) &= [0 \ 0 \ 1]^{\mathrm{T}} \ (\mathrm{m}), \ \bar{R}(0) = I. \end{aligned}$$

Let the reference of the rigid body motion (p_d, R_d) be given by

$$p_d = [0 \ 0 \ 1]^{\mathrm{T}} \ (\mathrm{m}), \ R_d = I.$$

Then, we would like to bring the actual relative rigid body motion (p, R) to the reference (p_d, R_d).

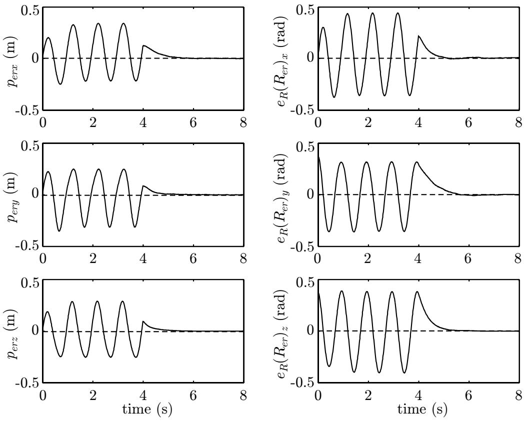

Fig. 5 Simulation results
($K_c = 24I$, $K_e = 2.4I$, $\gamma = 0.61$)

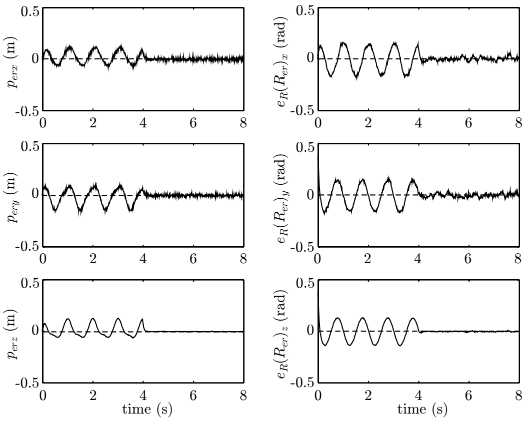

Fig. 6 Simulation results
($K_c = 72I$, $K_e = 24I$, $\gamma = 0.21$)

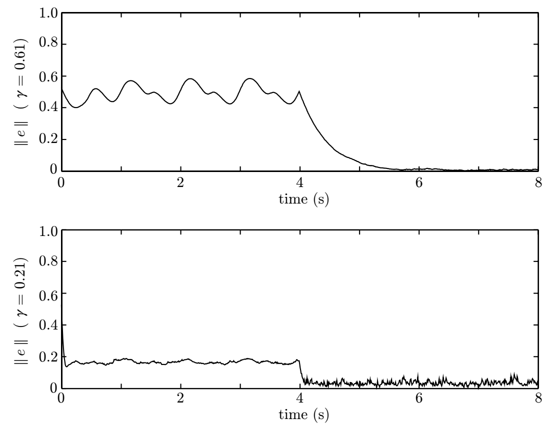

Fig. 7 Simulation results (Euclid norm of e)

Fig. 5 and Fig. 6 present the error vectors of the relative rigid body motion p_{er} and $e_R(R_{er})$ defined in the eq. (15). In Fig. 5 and Fig. 6, let p_{erx}, p_{ery} and p_{erz} denote the position error of the X-axis, the Y-axis and the X-axis, respectively. Similarly, $e_R(R_{er})_x$, $e_R(R_{er})_y$ and $e_R(R_{er})_z$ should be expressed.

Fig. 5 illustrates a case of the large $\gamma(=0.61)$ with $K_c = 24I$ and $K_e = 2.4I$. In contrast, Fig. 6 presents a case of the small $\gamma(=0.21)$ with $K_c = 72I$ and $K_e = 24I$. In the case of the static target object, i.e. after $t = 4$ [s], all errors in Fig. 5 and Fig. 6 tend to zero. It can be concluded that the equilibrium point is asymptotically stable if the target object is static.

On the other hand, there is a difference between the errors in Fig. 5 and the errors in Fig. 6 over the time interval $0 \le t < 4$ [s]. Fig. 7 shows the Euclid norm of the error vector e defined in (39), i.e. $\|e\|$. In Fig. 7, the upper side presents $\|e\|$ for $\gamma = 0.61$ and the lower side presents $\|e\|$ for $\gamma = 0.21$. In the case of $\gamma = 0.21$, the performance is improved as compared to the case of $\gamma = 0.61$. After all, the simulation results show that L_2-gain is adequate for the performance measure of the visual feedback control.

Since the camera model includes the nonlinearity (i.e. high order terms of the eq. (23) by using Taylor expansion) in the simulation, $J(\bar{p}, \bar{R})$ is not full column rank numerically if the gain matrices K_c and K_e are too large (e.g. $K_c = 100$, $K_e = 100$).

7. Conclusions

This paper has discussed stability and L_2-gain performance analysis for the full 3-D visual feedback system based on passivity from the theoretical standpoint. By using the representation of $SE(3)$, we have derived the relative rigid body motion dynamics between the moving target object and the camera. The nonlinear observer has been proposed in order to derive the visual feedback system. Based on passivity, stability and L_2-gain performance analysis have been performed. Especially, we made good use of the error function on $SO(3)$ as the Lyapunov or storage functions. Finally the simulation results have presented the effectiveness of the proposed controller and L_2-gain performance analysis. Our proposed passivity approach will enrich the field of visual servoing, although there are some problems which need to be considered. In particular, we expect to systematize the passivity based visual feedback control as well as the theory of the robot control based on the passivity approach. Future work will be devoted to discuss global stability and a region of attraction in the proposed method by using a path planning approach.

Acknowledgment

The author would like to thank the reviewers for their constructive comments and suggestions.

References

[1] S. Hutchinson, G. D. Hager, and P. I. Corke: A tutorial on visual servo control; *IEEE Trans. Robotics and Automation*, Vol. 12, No. 5, pp. 651–670 (1996)

[2] P. I. Corke and G. D. Hager: Vision-based robot control; *Control Problems in Robotics and Automation*, B. Siciliano and K. P. Valvanis Eds., Springer–Verlag, pp. 177–192 (1998)

[3] K. Hashimoto and H. Kimura: Visual servoing –Nonlinear observer approach–; *Journal of the*

Robotics Society of Japan, Vol. 13, No. 7, pp. 986–993 (1995)
[4] Y. Masutani and F. Miyazaki: Sensory feedback control for space manipulators; *Journal of the Robotics Society of Japan*, Vol. 7, No. 6, pp. 647–655 (1989)
[5] W. Wilson, C. Williams Hulls, and G. Bell: Relative end-effector control using cartesian position based visual servoing; *IEEE Trans. Robotics and Automation*, Vol. 12, No. 5, pp. 684–696 (1996)
[6] R. Kelly, R. Carelli, O. Nasisi, B. Kuchen, and F. Reyes: Stable visual servoing of camera-in-hand robotic systems; *IEEE Trans. Mechatronics*, Vol. 5, No. 1, pp. 39–48 (2000)
[7] O. Shakernia, Y. Ma, J. Koo, and S. S. Sastry: Landing an unmanned aerial vehicle: Vision based motion estimation and nonlinear control; *Asian Journal of Control*, Vol. 1, No. 3, pp. 128–145 (1999)
[8] E. Malis, F. Chaumette, and S. Boudet: 2-1/2-D Visual servoing; *IEEE Trans. Robotics and Automation*, Vol. 15, No. 2, pp. 238–250 (1999)
[9] N. J. Cowan and D. E. Koditschek: Planar image based visual servoing as a navigation problem; *Proc. 1999 IEEE Int. Conf. Robotics and Automation*, pp. 611–617 (1999)
[10] F. Conticelli and B. Allotta: Nonlinear controllability and stability analysis of adaptive image-based systems; *IEEE Trans. Robotics and Automation*, Vol. 17, No. 2, pp. 208–214 (2001)
[11] A. Maruyama and M. Fujita: Robust control for planar manipulators with image feature parameter potential; *Advanced Robotics*, Vol. 12, No. 1, pp. 67–80 (1998)
[12] A. Maruyama and M. Fujita: Stability and L_2-gain performance analysis for robust visual servo system; *Trans. IEE of Japan*, Vol. 118–C, No. 3, pp. 301–309 (1998)
[13] A. Maruyama and M. Fujita: Robust visual feedback control for robotic manipulator based on adaptive H_∞ control; *Trans. Inst. of Systems, Control and Information Eng.*, Vol. 12, No. 10, pp. 579–585 (1999)
[14] R. Murray, Z. Li, and S. S. Sastry: *A Mathematical Introduction to Robotic Manipulation*, CRC Press (1994)
[15] A. van der Schaft: *L_2-Gain and Passivity Techniques in Nonlinear Control* (2nd ed.), Springer–Verlag (2000)
[16] Y. Mezouar and F. Chaumette: Path planning in image space for robust visual servoing; *Proc. 2000 IEEE Int. Conf. Robotics and Automation*, pp. 2759–2764 (2000)
[17] H. Michel and P. Rives: Singularities in the determination of the situation of a robot effector from the perspective view of 3 points; *Technical Report*, INRIA (1993)
[18] F. Bullo and R. Murray: Tracking for fully actuated mechanical systems: a geometric framework; *Automatica*, Vol. 35, No. 1, pp. 17–34 (1999)

Appendix

Appendix 1. Model of Relative Rigid Body Motion

We shall derive the model of the relative rigid body motion presented in Section **2.1**. The property of the rotation matrix R, i.e. $RR^{\mathrm{T}}=I$, gives us

$$\dot{R}^{\mathrm{T}} = -R^{\mathrm{T}}\dot{R}R^{\mathrm{T}}. \tag{A1}$$

Differentiating (3) and (4) with respect to time, and using the above formula, we have

$$\begin{aligned}\dot{p} &= -R_{wc}^{\mathrm{T}}\dot{R}_{wc}R_{wc}^{\mathrm{T}}(p_{wo}-p_{wc}) + R_{wc}^{\mathrm{T}}(\dot{p}_{wo}-\dot{p}_{wc})\\ \dot{R} &= -R_{wc}^{\mathrm{T}}\dot{R}_{wc}R_{wc}^{\mathrm{T}}R_{wo} + R_{wc}^{\mathrm{T}}\dot{R}_{wo}.\end{aligned}$$

Substituting the eqs. (3) and (4) yields

$$\begin{aligned}\dot{p} &= -R_{wc}^{\mathrm{T}}\dot{R}_{wc}p + Rv_{wo} - v_{wc}\\ \dot{R} &= -R_{wc}^{\mathrm{T}}\dot{R}_{wc}R + R_{wc}^{\mathrm{T}}\dot{R}_{wo}.\end{aligned}$$

Using the eqs. (5) and (6), the above equations become

$$\begin{aligned}\dot{p} &= -R_{wc}^{\mathrm{T}}R_{wc}\hat{\omega}_{wc}p + Rv_{wo} - v_{wc}\\ &= -\hat{\omega}_{wc}p + Rv_{wo} - v_{wc} \qquad \text{(A2)}\\ \dot{R} &= -R_{wc}^{\mathrm{T}}R_{wc}\hat{\omega}_{wc}R + R_{wc}^{\mathrm{T}}R_{wo}\hat{\omega}_{wo}\\ &= -\hat{\omega}_{wc}R + R\hat{\omega}_{wo}. \qquad \text{(A3)}\end{aligned}$$

Recall that the operator '$\wedge$' implies the cross product; i.e., for two vectors $a,b\in\mathcal{R}^3$, $\hat{a}b=-\hat{b}a$ holds. Thus, from (A2), we can derive

$$\dot{p} = -v_{wc} + \hat{p}\omega_{wc} + Rv_{wo}. \tag{A4}$$

(A4) and (A3) are identical to (7) and (8), since (p,R) denotes (p_{co},R_{co}).

$R\hat{\omega}R^{\mathrm{T}} = (R\omega)^\wedge$ holds [14] (Chap.2, Lemma 2.1), where $R\in SO(3)$ and $\omega\in\mathcal{R}^3$. From (A3), this yields

$$\begin{aligned}\dot{R}R^{\mathrm{T}} &= -\hat{\omega}_{wc}RR^{\mathrm{T}} + R\hat{\omega}_{wo}R^{\mathrm{T}}\\ &= -\hat{\omega}_{wc} + (R\omega_{wo})^\wedge. \qquad \text{(A5)}\end{aligned}$$

By taking the operator '$\vee$' (vee) for (A5), we have

$$(\dot{R}R^{\mathrm{T}})^\vee = -\omega_{wc} + R\omega_{wo}.$$

Hence, (11) follows.

Appendix 2. Error Function on $SO(3)$

Let us introduce the notation of the error function.

$$\phi(R) := \frac{1}{2}\mathrm{tr}(I-R), \tag{A6}$$

and, for any 3×3 matrix A, $\mathrm{sk}(A) := \frac{1}{2}(A-A^{\mathrm{T}})$. The error function ϕ has the following properties.

Property 1 Let $R\in SO(3)$. The following properties hold.

(1) $\phi(R)=\phi(R^{\mathrm{T}})\geq 0$ and $\phi(R)=0$ if and only if $R=I$.

(2) $\dot{\phi}(R) = e_R^{\mathrm{T}}(R)(R^{\mathrm{T}}\dot{R})^\vee = e_R^{\mathrm{T}}(R)(\dot{R}R^{\mathrm{T}})^\vee$, where $e_R(R) := \mathrm{sk}(R)^\vee$.

These properties are proved in Ref. [18].

Appendix 3. Approximation of Feature Point

The approximation of feature point (27) will be derived. The eq. (22) can be rewritten as

$$p_{ci} = (p-\bar{p}) + \bar{p} + \bar{R}\bar{R}^{\mathrm{T}}Rp_{oi}$$

$$= p_{ee} + \bar{p} + \bar{R}R_{ee}p_{oi}. \tag{A7}$$

Suppose the estimation error is *small* enough that we can let $R_{ee} \simeq I + \mathrm{sk}(R_{ee})$ (which is derived from *Rodrigues' formula* in Ref. [14]), then the equation (A7) becomes

$$\begin{aligned} p_{ci} &= p_{ee} + \bar{p} + \bar{R}(I + \mathrm{sk}(R_{ee}))p_{oi} \\ &= \bar{p} + \bar{R}p_{oi} + \bar{R}\mathrm{sk}(R_{ee})p_{oi} + p_{ee} \\ &= \bar{p}_{ci} + \bar{R}\mathrm{sk}(R_{ee})p_{oi} + p_{ee} \end{aligned} \tag{A8}$$

where $\bar{p}_{ci} := \bar{p} + \bar{R}p_{oi}$. It should be noted that $\hat{a}b = -\hat{b}a, \forall a,b \in \mathcal{R}^3$ and $e_R(R) = \mathrm{sk}(R)^\vee, \forall R \in SO(3)$ hold, then we have

$$p_{ci} = \bar{p}_{ci} - \bar{R}\hat{p}_{oi}e_R(R_{ee}) + p_{ee}. \tag{A9}$$

Hence, (27) holds.

Appendix 4. State Equation of Estimation Error

Here we derive the state equation of the estimation error (36) in Section **3**.

Differentiating (25) with respect to time is

$$\dot{p}_{ee} = \dot{p} - \dot{\bar{p}} \tag{A10}$$

$$\begin{aligned} \dot{R}_{ee} &= \dot{\bar{R}}^{\mathrm{T}}R + \bar{R}^{\mathrm{T}}\dot{R} \\ &= -\bar{R}^{\mathrm{T}}\dot{\bar{R}}\bar{R}^{\mathrm{T}}R + \bar{R}^{\mathrm{T}}\dot{R}. \end{aligned} \tag{A11}$$

Substituting the eqs. (11) and (21) into (A10) yields

$$\dot{p}_{ee} = \left[\, 0 \;\; \hat{p}_{ee} \,\right] u_c - \left[\, I \;\; 0 \,\right] u_e + \left[\, R \;\; 0 \,\right] V_{wo}. \tag{A12}$$

Let $u_e = [v_{ue}^{\mathrm{T}} \; \omega_{ue}^{\mathrm{T}}]^{\mathrm{T}}$. Then $\dot{\bar{R}}$ can be derived from the eq. (21) as follows

$$\dot{\bar{R}} = -\hat{\omega}_{wc}\bar{R} + \bar{R}\hat{\omega}_{ue} \tag{A13}$$

which is similar to the eq. (A3).

Using the above equation and (A3), the eq. (A11) becomes

$$\begin{aligned} \dot{R}_{ee} &= -\bar{R}^{\mathrm{T}}(-\hat{\omega}_{wc}\bar{R} + \bar{R}\hat{\omega}_{ue})\bar{R}^{\mathrm{T}}R \\ &\quad + \bar{R}^{\mathrm{T}}(-\hat{\omega}_{wc}R + R\hat{\omega}_{wo}) \\ &= \bar{R}^{\mathrm{T}}\hat{\omega}_{wc}R - \hat{\omega}_{ue}R_{ee} - \bar{R}^{\mathrm{T}}\hat{\omega}_{wc}R + R_{ee}\hat{\omega}_{wo} \\ &= -\hat{\omega}_{ue}R_{ee} + R_{ee}\hat{\omega}_{wo}R_{ee}^{\mathrm{T}}R_{ee} \\ &= -\hat{\omega}_{ue}R_{ee} + (R_{ee}\omega_{wo})^\wedge R_{ee}. \end{aligned} \tag{A14}$$

Furthermore, the above equation can be rewritten as

$$(\dot{R}_{ee}R_{ee}^{\mathrm{T}})^\vee = -\omega_{ue} + R_{ee}\omega_{wo}. \tag{A15}$$

Thus, (36) holds.

**

丸山　章

1992 年金沢大学工学部電気・情報工学科卒業．1994 年北陸先端科学技術大学院大学情報科学研究科博士前期課程修了．同年（株）不二越入社．1999 年北陸先端科学技術大学院大学情報科学研究科博士後期課程修了．現在，ロボット事業部開発部に所属．計測自動制御学会などの会員．

河合　宏之 (学生会員)

1999 年金沢大学工学部電気・情報工学科卒業．2001 年金沢大学大学院博士前期課程修了，同年金沢大学大学院博士後期課程入学，現在に至る．計測自動制御学会の会員．

藤田　政之 (正会員)

1984 年早稲田大学大学院理工学研究科博士前期課程修了（電気工学専攻），1985 年同博士後期課程中退．同年金沢大学工学部電気・情報工学科助手．同講師，助教授を経て，1992 年北陸先端科学技術大学院大学情報科学研究科助教授．1999 年金沢大学工学部電気・情報工学科教授．ロバスト制御とその応用に関する研究に従事．工学博士．計測自動制御学会，IEEE などの会員．